STATISTICS, OPTIMIZATION AND INFORMATION COMPUTING
Stat., Optim. Inf. Comput., Vol. **x**, Month 202x, pp 0–15.
Published online in International Academic Press (www.IAPress.org)

A Study on Partition-Based Resolving Parameters in Molecular Graphs of Anticancer Drugs

M. Donganont [1], R. Nithya Raj [2,*], P. Selvarani [3], M. Rajasekar [4], S. Rajeshwari [5]

[1] *School of Science, University of Phayao, 56000, Thailand*
[2] *Department of Mathematics, Hindustan Institute of Technology and Science, Chennai - 603103, India*
[3] *Department of Mathematics, SRM Institute of Science and Technology, Trichy - 621105, India*
[4] *Department of Computer Science, Saveetha College of Liberal Arts and Sciences, SIMATS University, Chennai - 602105, India*
[5] *Department of Mathematics, St. Joseph's Institute of Technology, OMR, Chennai - 600119, India*

Abstract Cancer remains one of the most life-threatening diseases worldwide, and effective therapeutic options are still limited for several cancer types. Recently, HDAC-based multitarget anti- cancer drugs have attracted considerable attention due to their promising biological activity. In chemical graph theory, drug molecules are often represented using graph models, where atoms correspond to vertices and the chemical bonds between them are depicted as edges. One important graph invariant is the partition dimension, which measures the minimum number of vertex partitions required to uniquely determine the position of every vertex in a graph based on distance representations. In this paper, we investigate the partition dimension of molecular graphs corresponding to the anticancer drugs vorinostat, tucidinostat, triciferol, CUDC-101, and CUDC-907. These drugs play a significant role in modern cancer therapy, particularly in epigenetic and multitarget treatments. In the current study we build chemical graph models of the compounds under study, solve appropriate resolving partitions, and give accurate value or bounds of these partition dimensions. The results show that partition dimension provides an effective and sparse structure of distinctly identifying atomic locations in complicated drug molecules, thus highlighting its applicability as a potent structural label of anticancer molecules and enhancing the interdisciplinary discussion between graph theory and medicinal chemistry.

Keywords Partition dimension, resolving partitions, anticancer drugs, molecular graphs, drug structure analysis

AMS 2010 subject classifications 05C12, 05C25

DOI: 10.19139/soic-2310-5070-3988

1. Introduction

Cancer is conventionally characterized by an uncontrolled growth of abnormal cells of the human body, which is usually triggered by contact with carcinogenic factors. These agents like some organic compounds present in cigarette smoke and tobacco products promote the metastatic proliferation of numerous body systems. The disease has no specific clinical signs, shows its nonspecific manifestations in the form of palpable masses, incorrect bleeding, persistent cough, and weight loss without a defined cause. Major contributors to cancer risk include smoking, excess body weight, poor dietary habits, physical inactivity, and heavy alcohol consumption, all of which significantly elevate oncogenic potential. Current treatment approaches encompass surgical procedures, radiation therapy, cytotoxic chemotherapy, hormone-based therapies, and advanced targeted treatments.

CUDC-101 is a multi-target anticancer agent whose molecular formula is $C_{24}H_{26}N_4O_4$ as shown in Figure 1. It functions as an inhibitor of histone deacetylase (HDAC) and may be useful in treating a number of cancers,

*Correspondence to: Nithya Raj. R (Email: nithyarajmaths@gmail.com). Department of Mathematics, Hindustan Institute of Technology and Science, Chennai (603103), India.

ISSN 2310-5070 (online) ISSN 2311-004X (print)

including liver, breast, and stomach cancer [1]. Clinical and experimental research also shows that CUDC-101 has an increased radiosensitizing effect relative to vorinostat especially in the pancreatic cancer treatment [2].

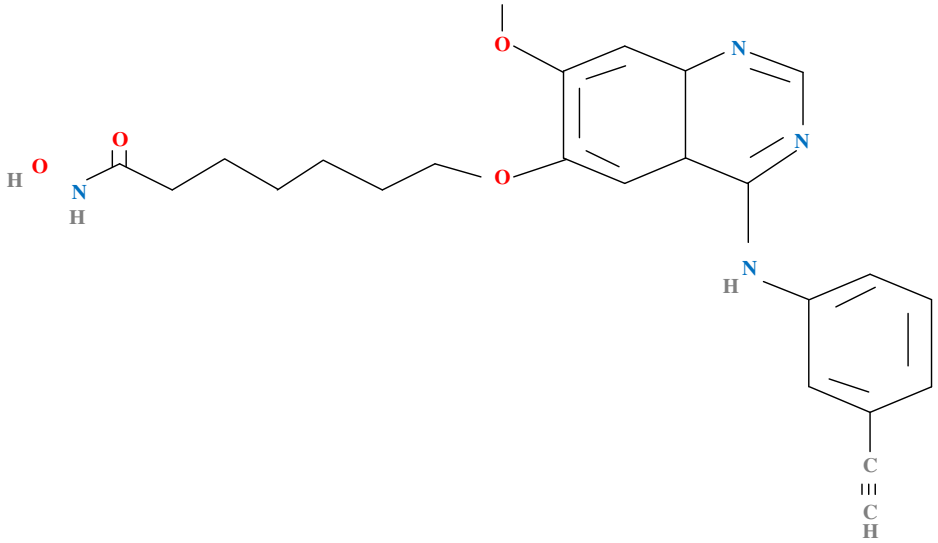

Figure 1. The molecular structure of CUDC-101

CUDC-907 is a dual HDAC inhibitor of molecular composition $C_{23}H_{24}N_8O_4$ as seen in Figure 2. This agent has been known to be a potent molecularly targeted anticancer compound [3]. It has also been tested in clinical and pre-clinical trials to treat a wide range of malignancies, such as multiple myeloma, breast cancer, lymphoma, NUT midline carcinoma, and a number of solid tumors [1].

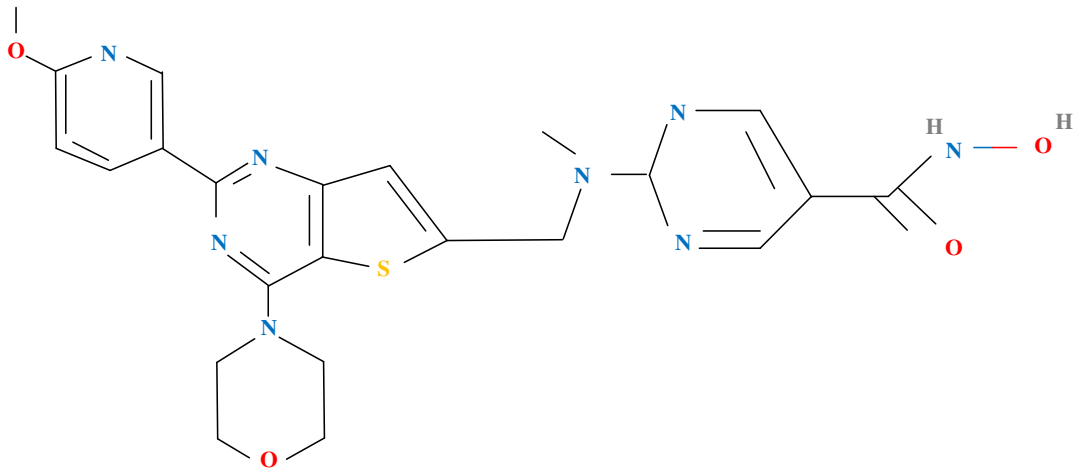

Figure 2. The CUDC-907 chemical structures

Zolinza (also known as vorinostat) is an anticancer agency which is approved to treat cutaneous T influenza cell lymphoma. It is an artificial hydroxamic acid-based acid which has antineoplastic effects by binding to the catalytic site of histone deacetylase (HDAC) enzymes [4]. Vorinostat is a drug that is administered orally and is an HDAC inhibitor. The molecular structure of vorinostat is displayed in Figure 3. The formula for its molecules is $C_{14}H_{20}N_2O_3$ [1].

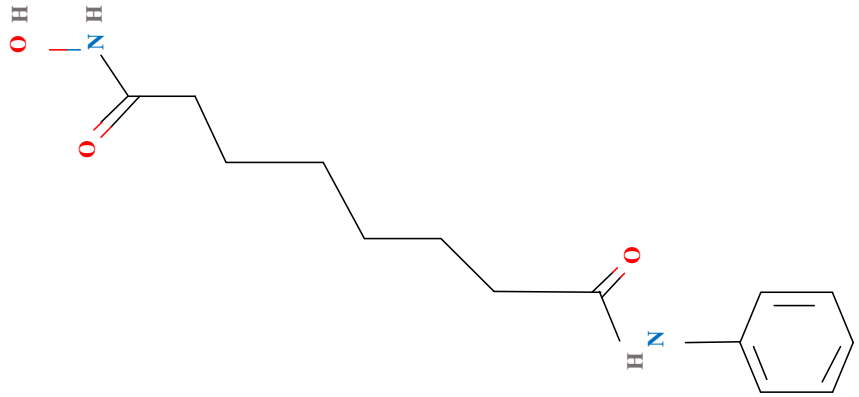

Figure 3. The vorinostat's chemical structure

Tucidinostat is an orally administered histone deacetylase inhibitor belonging to the benzamide class, with the molecular formula is $C_{22}H_{19}FN_4O_2$. The chemical structure of tucidinostat are presented in Figure 4. The medicine has been used to treat lymphomas and other solid cancers [1].

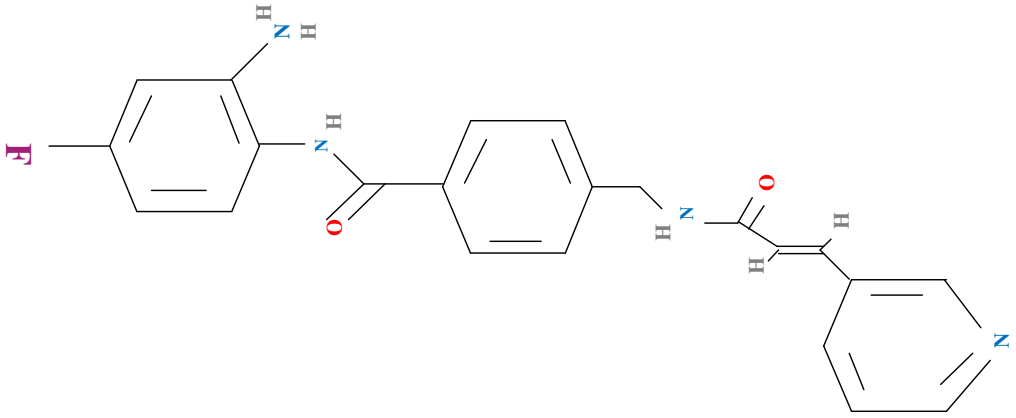

Figure 4. The tucidinostat's chemical structure

Triciferol is a hybrid anticancer compound with the molecular formula is $C_{26}H_{39}NO_4$. It demonstrates strong antiproliferative and cytotoxic effects in multiple in vitro cancer cell models. This drug integrates vitamin D receptor (VDR) agonist activity with histone deacetylase (HDAC) inhibitory properties [5]. Figure 5 shows the molecular structure of triciferol. The physicochemical parameters, including density (D), molar refraction (MR), LogP, polar surface area (PSA), polarizability (P), surface tension (T), and molar volume (MV), for the drugs CUDC-907, CUDC-101, triciferol, vorinostat, and tucidinostat were retrieved from the Chemspider database. Selected values of these properties are summarized in Table 1.

In this work, a molecular graph is obtained by representing a chemical structure as a graph in which atoms correspond to vertices and chemical bonds correspond to edges. This graph-theoretic representation is well established in the literature, and further details can be found in recent studies [6–10].

Cancer remains one of the leading causes of morbidity and mortality worldwide, necessitating the continuous development of novel and more effective therapeutic agents. In recent years, epigenetic modulators and multi-targeted inhibitors such as vorinostat, tucidinostat, triciferol, CUDC-101, and CUDC-907 have emerged as promising anticancer drugs due to their enhanced efficacy and reduced resistance profiles. Vorinostat and tucidinostat are histone deacetylase (HDAC) inhibitors that regulate gene expression and induce apoptosis in

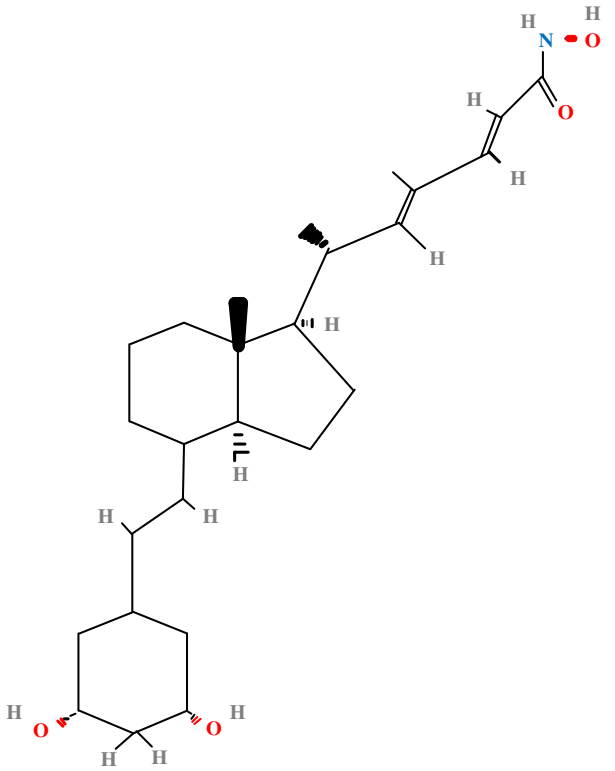

Figure 5. Molecular structure of triciferol

Table 1. Physicochemical characteristics of specific anticancer medications [5]

Property	**CUDC-907**	**CUDC-101**	**Triciferol**	**Vorinostat**	**Tucidinostat**
Density	1.4	1.3	1.1	1.2	1.3
Molar refraction	135.3	121.1	122.0	73.5	111.8
LogP	2.39	2.84	5.53	0.86	2.40
Polar surface area	167	106	52	78	97
Polarizability	53.7	48.0	48.4	29.1	44.3
Surface tension	78.3	67.8	43.9	50.4	62.7
Molar volume	351.8	337.2	387.0	225.0	292.0

various malignancies, including breast, lung, and hematological cancers. Triciferol, a hybrid vitamin-D receptor-based compound, exhibits strong antiproliferative and cytotoxic activity against multiple cancer cell lines. CUDC-101 and CUDC-907 are dual-function inhibitors targeting HDACs along with key oncogenic signaling pathways such as EGFR, PI3K, and Akt, thereby suppressing tumor growth and progression more effectively than single-target drugs. These novel agents have shown significant potential in preclinical and clinical studies and represent an important advancement in targeted and combination cancer therapy strategies [11–15].

The remaining sections of the paper are divided as follows. Section 2 provides preliminary information and fundamental concepts, while Section 3 lists the key conclusions. Section 4 contains the last observation of the results, while Section 5 discusses the conclusion and future directions.

2. Basic concepts

This section presents the basic concepts, definitions, theorems, symbols, and terminology used throughout the paper. These preliminaries provide the necessary graph-theoretical background for the subsequent analysis of the partition dimension of the considered anticancer drug molecular graphs.

Definition 2.1. Let G be a connected graph and let $u, v \in V(G)$. The *distance* between u and v, denoted by $d(u, v)$, is defined as the length of a shortest u–v path in G. In other words, $d(u, v)$ is the minimum number of edges among all paths connecting u and v.

Definition 2.2. Let $R = \{a_1, a_2, \ldots, a_k\}$ be an ordered subset of the vertex set $V(G)$ of a graph G. For any vertex $p \in V(G)$, the metric representation of p with respect to R is defined as the k-tuple $r(p \mid R) = \big(d(p, a_1), d(p, a_2), \ldots, d(p, a_k)\big)$. The set R is called a resolving set of G if the metric representations $r(p \mid R)$ are distinct for all vertices $p \in V(G)$. A resolving set with minimum cardinality is known as a metric basis, and its cardinality is referred to as the metric dimension of the graph G and it is denoted by $dim(G)$.

Definition 2.3. Let G be a connected graph and let $\pi = \{\pi_1, \pi_2, \pi_3, \ldots, \pi_k\}$ be an ordered partition of the vertex set of $V(G)$. For any vertex $\alpha \in V(G)$, the partition representation of α with respect to π is defined as $r(\alpha \mid \pi) = \big(d(\alpha, \pi_1), d(\alpha, \pi_2), d(\alpha, \pi_3), \ldots, d(\alpha, \pi_k)\big)$, where $d(\alpha, \pi_i) = \min\{d(\alpha, x) : x \in \pi_i\}$ for $1 \leq i \leq k$. If each vertex's partition representation is unique, then the partition π is referred to as a resolving partition of G. A resolving partition with minimum cardinality is referred to as a minimum resolving partition, and its cardinality is called the partition dimension of the graph G and it is denoted by the term $pd(G)$.

Definition 2.4. The *Kronecker delta* associated with a set S is defined by

$$\delta_r = \begin{cases} 1, & \text{if } r \in S, \\ 0, & \text{if } r \notin S. \end{cases}$$

Theorem 2.5. [18] *Let $x_1, x_2 \in V(G)$, and let π be a resolving partition of $V(G)$. If for all nodes $y \in V(G) \setminus \{x_1, x_2\}$, the distance representations of x_1 and x_2 with respect to π are distinct, then x_1 and x_2 must belong to different partition classes in π.*

Theorem 2.6. [18] *Consider a connected simple graph G that contains no isolated vertices.*
(i) The partition dimension $pd(G)$ equals 2 if and only if G is a path graph with at least 2 vertices.
(ii) The partition dimension $pd(G)$ is equal to t if and only if G is isomorphic to the complete graph K_t.

Theorem 2.7. [18] *Let G be any connected graph with at least two vertices. Then, the partition dimension $pd(G)$ and the metric dimension $\dim(G)$ satisfy the inequality $pd(G) \leq \dim(G) + 1$.*

To provide a clear overview of the procedure for determining the resolving partition sets of the molecular drug structures, a flowchart illustrating the complete methodology is presented in Figure 6.

The number of symbols and notations in relation to metrics and their generalizations are listed in Table 2. The literature that is presented in the text explains a range of applications for these concepts.

In graph theory, resolvability describes the property by which vertices of a graph can be uniquely distinguished using their distance relationships to a chosen collection of reference vertices. In 1975, Slater [16] introduced the notion of a resolving set for connected graphs, referring to it as a locating set because of its connection to problems involving the unique identification of intruder locations in networks. He also demonstrated the applicability of this concept to navigation and detection systems such as LORAN and SONAR stations. In 1976, Harary and Melter [17] independently studied the same concept, introducing the term metric dimension in place of the previously used location number. In the context of pure graph theory, this concept is commonly referred to as a metric basis and has been extensively studied in the literature [18, 19]. Concepts of resolvability have found wide-ranging applications across several fields, such as combinatorial optimization, robotic navigation, complex game theory, image processing, pharmaceutical chemistry, polymer synthesis, and electromagnetic field analysis. Detailed discussions of these applications can be found in [17, 20–23].

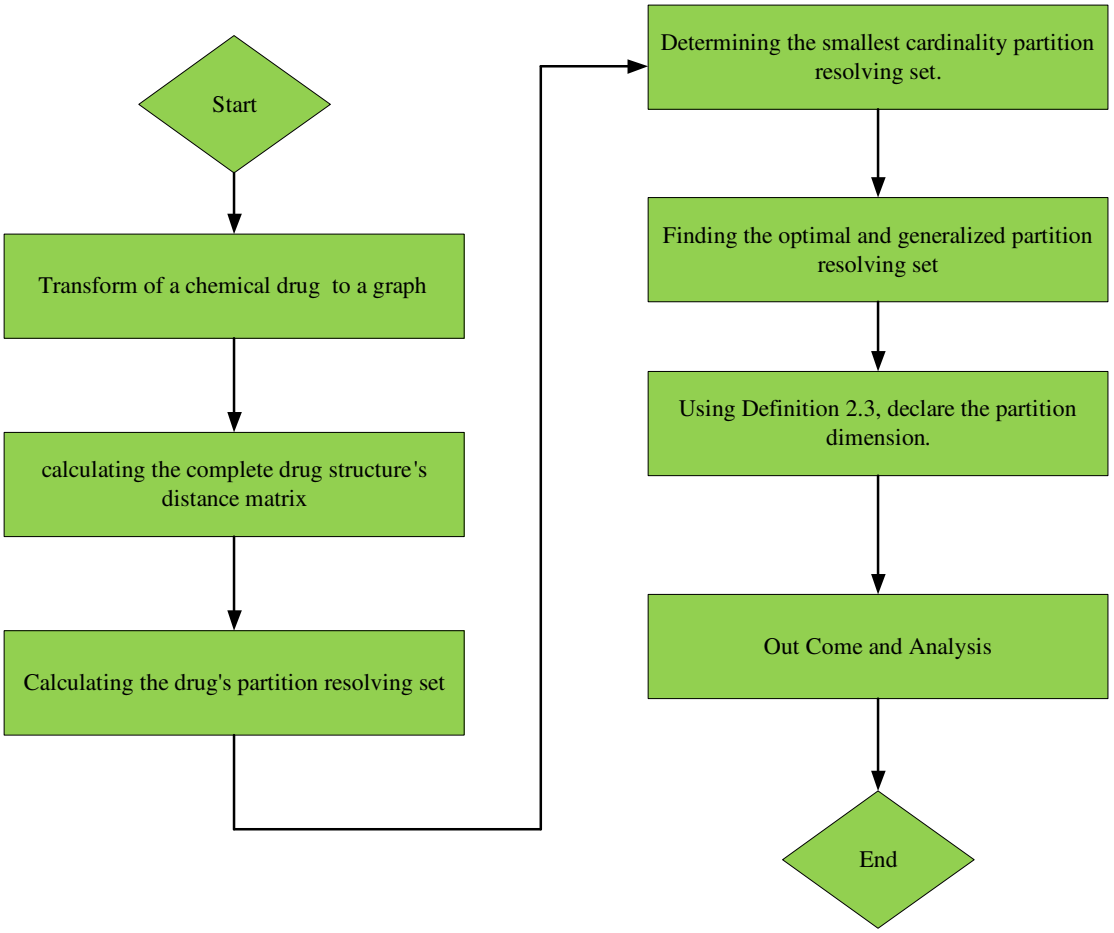

Figure 6. Flowchart to calculate a chemical structure's partition dimension

Rather than selecting a single subset of vertices, the authors in [19] proposed an alternative approach in which the entire vertex set of a graph is divided into mutually disjoint subsets. This partitioning is carried out so that each vertex can be uniquely identified through distance information, giving rise to the notion of a resolving partition and the associated parameter known as the partition dimension. The partition dimension is a vertex-based graph invariant, closely related to the metric dimension. Determining the metric dimension of various chemical graph structures is known to be an NP-hard problem, and the computation of the partition dimension shares the same level of computational complexity. Owing to its inherently more intricate structure compared to the metric dimension, the partition dimension admits fewer exact resolving partitions, and consequently, results are often expressed in terms of bounds rather than precise values.

The partition dimension exhibits a higher level of structural complexity compared to the metric dimension; as a result, exact resolving partitions are relatively rare, and most investigations focus on establishing upper and lower bounds. Bounds for the partition dimension of generalized families of convex polytopes have been reported in [24, 25]. Further studies have explored chemical graph models, including fullerene structures [26] and other molecular networks with derived bounds [27]. Partition-based descriptions of various nanotube and nanosheet configurations were examined in [28], while two-dimensional lattice frameworks were discussed in [29]. The study of the central local metric dimension for corona product graphs and the dominant local metric dimension has been presented in [30, 31]. In [32], the partition dimension of COVID-19 antiviral drug molecules is analyzed,

whereas [33] focuses on the partition resolvability of chemical structures related to breast cancer. In [34–40], generalized structures and classes of graph families are described in depth.

Table 2. Symbols and Terminology Used Throughout the Paper

Meaning	**Symbol**
Graph representing the molecular framework	G
Set of all vertices of G	$V(G)$
Set of all edges of G	$E(G)$
Locating (resolving) vertex subset	L
Cardinality of a locating set	$\|L\|$
Partition resolving number of G	$pd(G)$
Partition resolving family of G	π
A vertex x's distance representation with regard to π	$r(x\|\pi)$

3. Anticancer Drugs and their Partition Resolving Number

The main findings on the partition resolving sets for the chemical graph structures of CUDC-101, CUDC-907, Triciferol, Vorinostat, and Tucidinostat are summarized in this section.

Theorem 3.1. *Let $G_{CUDC101}$ be a novel drug structure then, $pd(G_{CUDC101}) = 3$.*

Proof. The chemical graph of $CUDC101$ has 32 total nodes, also known as the order, and 34 total edges, also known as the size. The vertex and edge set of $CUDC101$ drug structure defined by $V(G_{CUCD101}) = \{c_r : 1 \leq r \leq 32\}$, $E(G_{CUDC101}) = \{c_r c_{r+1} : 1 \leq r \leq 19\} \cup \{c_r c_{r+1} : 21 \leq r \leq 22\} \cup \{c_{18}c_{23}\} \cup \{c_r c_{r+1} : 24 \leq r \leq 25\} \cup \{c_{24}c_{27}\} \cup \{c_r c_{r+1} : 27 \leq r \leq 30\} \cup \{c_{16}c_{21}\} \cup \{c_3 c_{32}\} \cup \{c_{11}c_{24}\} \cup \{c_{13}c_{28}\} \cup \{c_{14}c_{31}\}$.

Table 3. Representation of each node of $G_{CUDC101}$ with respect π

$r(c_r\|\pi)$	π_1	π_2	π_3	Range
c_r	0	19	δ_r	$r = 1$
c_r	$r-1$	$n-12-r$	0	$2 \leq r \leq 19$
c_r	19	0	δ_r	$r = 20$
c_r	$r-5$	$n-6-r$	0	$21 \leq r \leq 23$
c_r	$r-13$	$r-14$	0	$24 \leq r \leq 26$
c_r	$n-15$	$n+r-6$	0	$27 \leq r \leq 30$
c_r	14	7	0	$r = 31$
c_r	3	18	0	$r = 32$

Additionally, Figure 7 shows the molecular graph of the CUDC 101 drug structure and labeling used to demonstrate our main conclusions. Therefore, 3 is the partition resolving number of $G_{CUDC101}$.

Let $\pi = \{\pi_1, \pi_2, \pi_3\}$ where $\pi_1 = \{c_1\}$ $\pi_2 = \{c_{20}\}$, and $\pi_3 = V(G_{CUDC101}) \setminus \{\pi_1 \cup \pi_2\}$. We assert that π constitutes a partition resolving set of the graph $G_{\text{CUDC 101}}$. To establish this, it is sufficient to verify that each vertex c_r, for $1 \leq r \leq 32$, possesses a unique distance representation relative to the partition π. The distance representations of all vertices of $G_{\text{CUDC 101}}$ are displayed in Table 3 with respect to π.

$$\delta_r = \begin{cases} 1, & \text{if } r \in \{1, 20\}, \\ 0, & \text{otherwise.} \end{cases}$$

Considering the identification $r(c_r \mid \pi)$, all vertices of the CUDC-101 drug structure can be uniquely recognized, which confirms that the partition π is a partition resolving set. This determined the partition resolving number of the

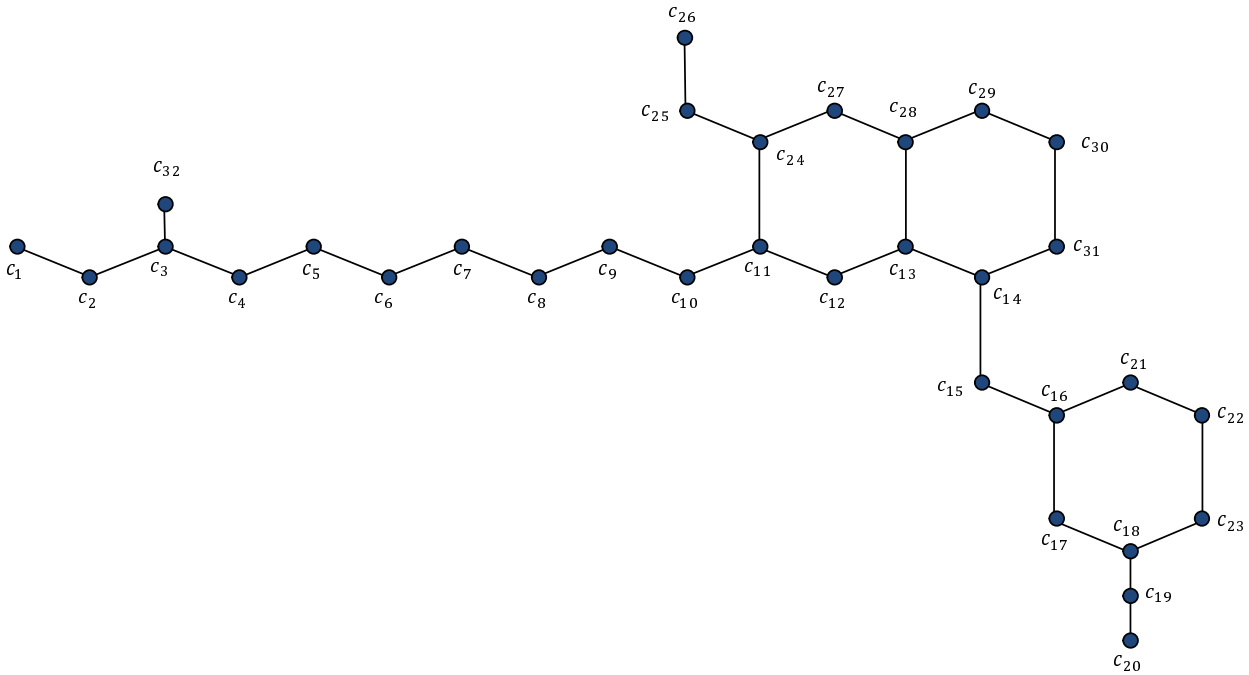

Figure 7. The CUDC-101 chemical graph

CUDC 101 drug structure graph, $pd(G_{CUDC101}) \leq 3$. By Theorem 2.6, we have $pd(G_{CUDC101}) \geq 3$. Combining this result with the previously established upper bound, we conclude that $pd(G_{CUDC101}) = 3$.

Theorem 3.2. *Let $G_{CUDC907}$ be a novel drug structure then, $pd(G_{CUDC907}) \leq 4$.*

Proof. The chemical graph of $CUDC907$ contains 40 total edges, or size, and 36 total nodes, or order. The vertex and edge set of CUDC 907 drug structure defined by $V(G_{CUCD-907}) = \{u_r : 1 \leq r \leq 36\}$, $E(G_{CUDC907}) = \{u_r u_{r+1} : 1 \leq r \leq 20\} \cup \{u_r u_{r+1} : 22 \leq r \leq 23\} \cup \{u_r u_{r+1} : 25 \leq r \leq 26\} \cup \{u_i u_{r+1} : 30 \leq r \leq 31\} \cup \{u_{16}u_{28}\} \cup \{u_{28}u_{29}\} \cup \{u_{19}u_{29}\} \cup \{u_{13}u_{22}\} \cup \{u_{24}u_{27}\} \cup \{u_{22}u_{25}\} \cup \{u_3u_{35}\} \cup \{u_4u_{33}\} \cup \{u_{33}u_{34}\} \cup \{u_7u_{34}\} \cup \{u_8u_{36}\} \cup \{u_{10}u_{30}\} \cup \{u_{32}u_{15}\} \cup \{u_{12}u_{31}\}$.

Moreover, Figure 8 illustrates the chemical graph of the CUDC 907 drug, along with the vertex labeling adopted to establish our main results. As a result, $G_{CUDC907}$ has a partition resolving number of less than or equal to 4.

Consider the partition $\pi = \{\pi_1, \pi_2, \pi_3, \pi_4\}$ where $\pi_1 = \{u_1\}$ $\pi_2 = \{u_{23}\}$, $\pi_3 = \{u_6, u_{28}\}$, and $\pi_4 = V(G_{CUDC907}) \setminus \{\pi_1 \cup \pi_2 \cup \pi_3\}$. We claim that π serves as a partition resolving set for the graph $G_{\text{CUDC 907}}$. To justify this claim, it suffices to verify that every vertex u_r, for $1 \leq r \leq 36$, admits a distinct distance representation with respect to the partition π. The corresponding representations of the vertices of $G_{\text{CUDC 907}}$ are listed in Table 4.

$$\delta_r = \begin{cases} 1, & r \in \{1, 6, 23, 28\}, \\ 0, & r \notin \{1, 6, 23, 28\}. \end{cases}$$

Under the identification $r(u_r \mid \pi)$, each vertex of the CUDC907 drug structure is uniquely distinguished and hence satisfies the definition of a partition resolving set. As a result, $pd(G_{CUDC907}) \leq 4$ is satisfied by the partition resolving number of the graph connected to the CUDC907 drug structure.

Theorem 3.3. *Let $G_{Varinostat}$ be a novel drug structure then, $pd(G_{Varinostat}) = 3$.*

Proof. The chemical graph of varinostat has 19 total nodes, also known as the order, and 19 total edges, also known as the size. The vertex and edge set of varinostat drug structure defined by $V(G_{varinostat}) = \{v_r : 1 \leq r \leq 19\}$, $E(G_{varinostat}) = \{v_r v_{r+1} : 1 \leq r \leq 13\} \cup \{v_{12}v_{16} \cup \{v_{16}v_{17}\} \cup \{v_{15}v_{17} \cup \{v_{10}v_{18}\} \cup \{v_3v_{19}\}$.

Table 4. Representation of each node of $G_{CUDC907}$ with respect to π

$r(u_r\|\pi)$	π_1	π_2	π_3	π_4	Range
u_r	0	14	5	δ_r	$r=1$
u_r	$r-1$	$n-21-r$	$n-30-r$	0	$2\leq r\leq 5$
u_i	$r-1$	9	0	δ_r	$r=6$
u_r	$r-1$	$n-21-i$	$n-42+r$	0	$7\leq r\leq 11$
u_r	$r-1$	$n-21-r$	$n-19-r$	0	$r=12,13$
u_r	$r-1$	3	3	0	$r=14$
u_r	$r-2$	4	2	0	$r=15$
u_r	$r-2$	$n-47+r$	$n-51+r$	0	$16\leq r\leq 18$
u_r	$r-2$	8	2	0	$r=19$
u_r	$r-2$	$n-47+r$	$n-53+r$	0	$r=20,21$
u_r	13	1	5	0	$r=22$
u_r	14	0	6	δ_r	$r=23$
u_r	15	1	7	0	$r=24$
u_r	$n+r-47$	$n+r-59$	$n+r-55$	0	$25\leq r\leq 26$
u_r	16	2	8	0	$r=27$
u_r	15	6	0	δ_r	$r=28$
u_r	16	7	1	0	$r=29$
u_r	$n+r-56$	$n-r-1$	$n-r-1$	0	$30\leq r\leq 31$
u_r	12	5	3	0	$r=32$
u_r	$n+r-65$	$n+7-r$	$n-r$	0	$33\leq r\leq 34$
u_r	3	13	4	0	$r=35$
u_r	8	8	3	0	$r=36$

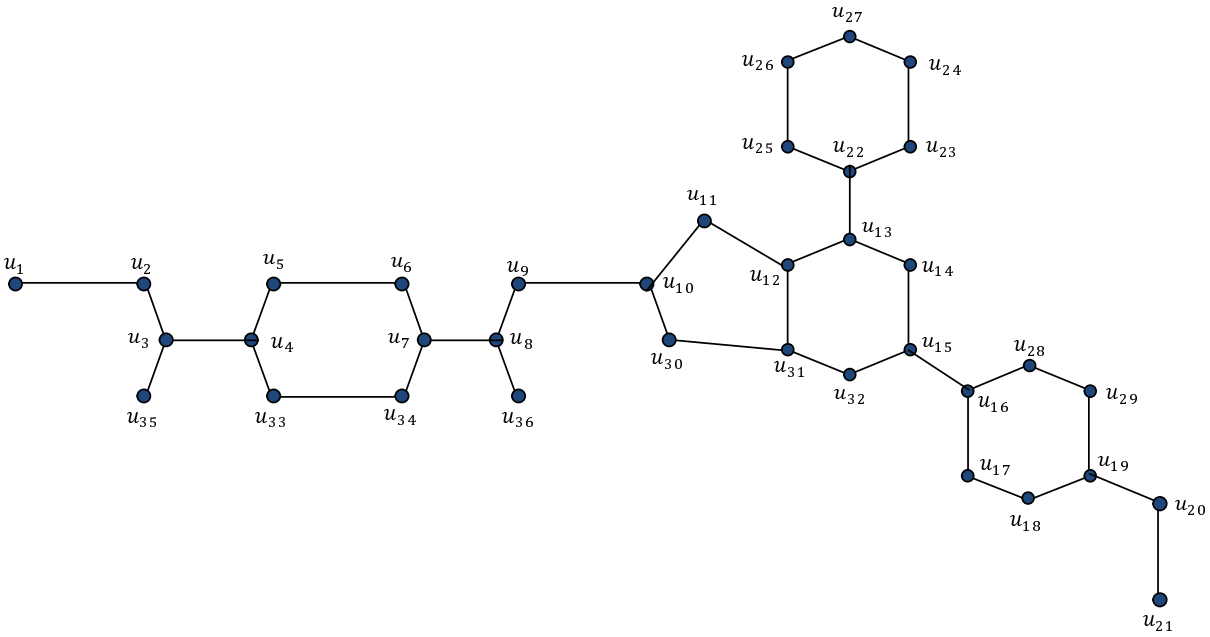

Figure 8. The CUDC-907 chemical graph

Moreover, Figure 9 depicts the chemical graph of the varinostat drug, together with the vertex labeling employed to derive our main results. Consequently, 3 is the partition resolving number of $G_{\text{varinostat}}$.

Let $\pi = \{\pi_1, \pi_2, \pi_3\}$ where $\pi_1 = \{v_1\}$ $\pi_2 = \{v_{17}\}$, and $\pi_3 = V(G_{varinostat}) \setminus \{\pi_1 \cup \pi_2\}$. We assert that π forms a partition resolving set for the graph $G_{\text{varinostat}}$. To confirm this assertion, it is sufficient to check that every vertex v_r, for $1 \leq r \leq 19$, possesses a unique distance representation relative to the partition π. The distance representations of the vertices of $G_{\text{varinostat}}$ with respect to π are summarized in Table 5.

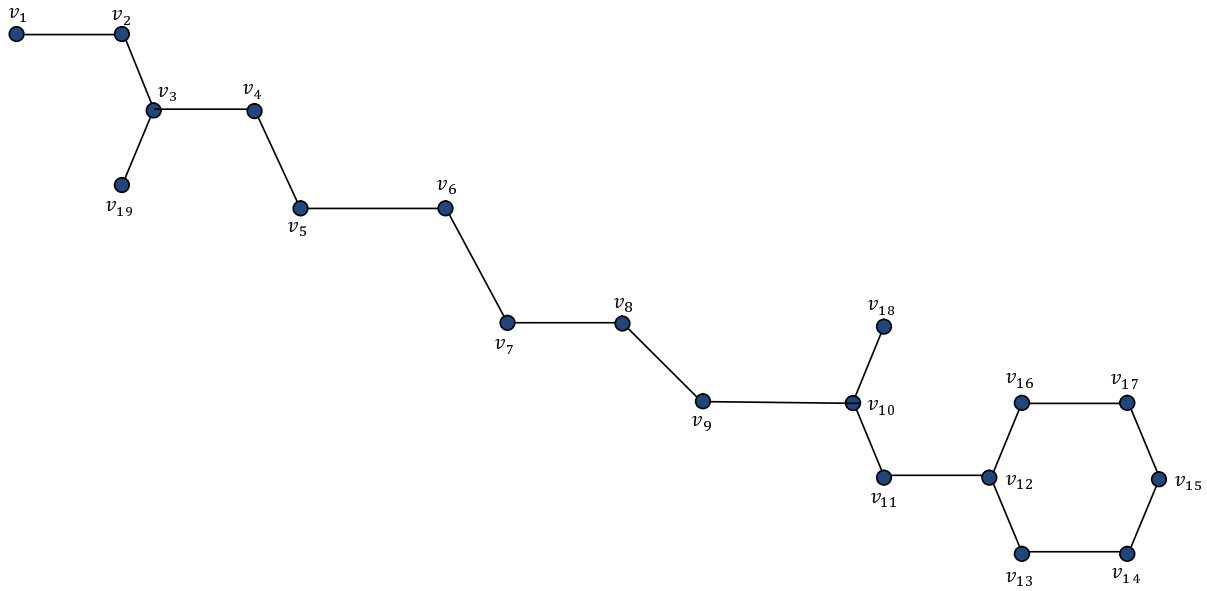

Figure 9. The vorinostat's chemical graph

Table 5. Representation of each node of vorinostat with respect π

$r(v_r\|\pi)$	π_1	π_2	π_3	Range
v_r	0	13	δ_r	$r = 1$
v_r	$r-1$	$n-r-5$	0	$2 \leq r \leq 12$
v_r	$n-20+r$	$n-3-r$	0	$13 \leq r \leq 14$
v_r	$n-23+r$	$n-2-r$	0	$r = 16$
v_r	13	0	δ_r	$r = 17$
v_r	$n-19$	$\frac{n-9}{2}$	0	$r = 18$
v_r	$n-16$	$4(n-16)$	0	$r = 19$

$$\delta_r = \begin{cases} 1, & r \in \{1, 17\}, \\ 0, & r \notin \{1, 17\}. \end{cases}$$

In identification $r(v_r \mid \pi)$, each vertex of the Vorinostat drug structure is uniquely determined and thus satisfies the conditions of a partition resolving set. Consequently, the partition resolving number of the graph corresponding to the Vorinostat drug structure is $pd(G_{vorinostat}) \leq 3$. By Theorem 2.6, we have $pd(G_{vorinostat}) \geq 3$. Combining this result with the previously established upper bound, we conclude that $pd(G_{vorinostat}) = 3$.

Theorem 3.4. *Let $G_{Tucidinostat}$ be a novel drug structure then, $pd(G_{Tucidinostat}) = 3$.*

Proof. The chemical graph of Tucidinostat has 29 total nodes, also known as the order, and 31 total edges, also known as the size. The vertex and edge set of Tucidinostat drug structure defined by $V(G_{Tucidinostat}) = \{v_r : 1 \leq r \leq 29\}$, $E(G_{Tucidinostat}) = \{t_r t_{r+1} : 1 \leq r \leq 17\} \cup \{t_{19}t_{15} \cup \{t_{19}t_{20}\} \cup \{t_{18}t_{20}\} \cup \{t_r t_{r+1} : 21 \leq r \leq 22\} \cup \{t_2 t_{21}\} \cup \{t_{22}t_{24}\} \cup \{t_{24}t_{25}\} \cup \{t_3 t_{25}\} \cup \{t_9 t_{27}\} \cup \{t_5 t_{29}\} \cup \{t_{12}t_{28}\} \cup \{t_{26}t_{27}\} \cup \{t_6 t_{26}\}$.

Further, Figure 10 displays the Tucidinostat drug structure and labeling molecular graph that we used to illustrate our main findings. Thus, $G_{Tucidinostat}$ has a partition resolving number of 3.

Let $\pi = \{\pi_1, \pi_2, \pi_3\}$, where $\pi_1 = \{t_1\}$, $\pi_2 = \{t_{19}, t_{27}\}$, and $\pi_3 = V(G_{\text{Tucidinostat}}) \setminus (\pi_1 \cup \pi_2)$, be a partition of the vertex set of $G_{\text{Tucidinostat}}$. Validating that every vertex t_r, for $1 \leq r \leq 29$, in $G_{\text{Tucidinostat}}$ permits a unique representation with regard to π is sufficient to prove that π is a partition resolving set. The corresponding representations c_r of the vertices of $G_{\text{Tucidinostat}}$, for $1 \leq r \leq 29$, are presented in Table 6.

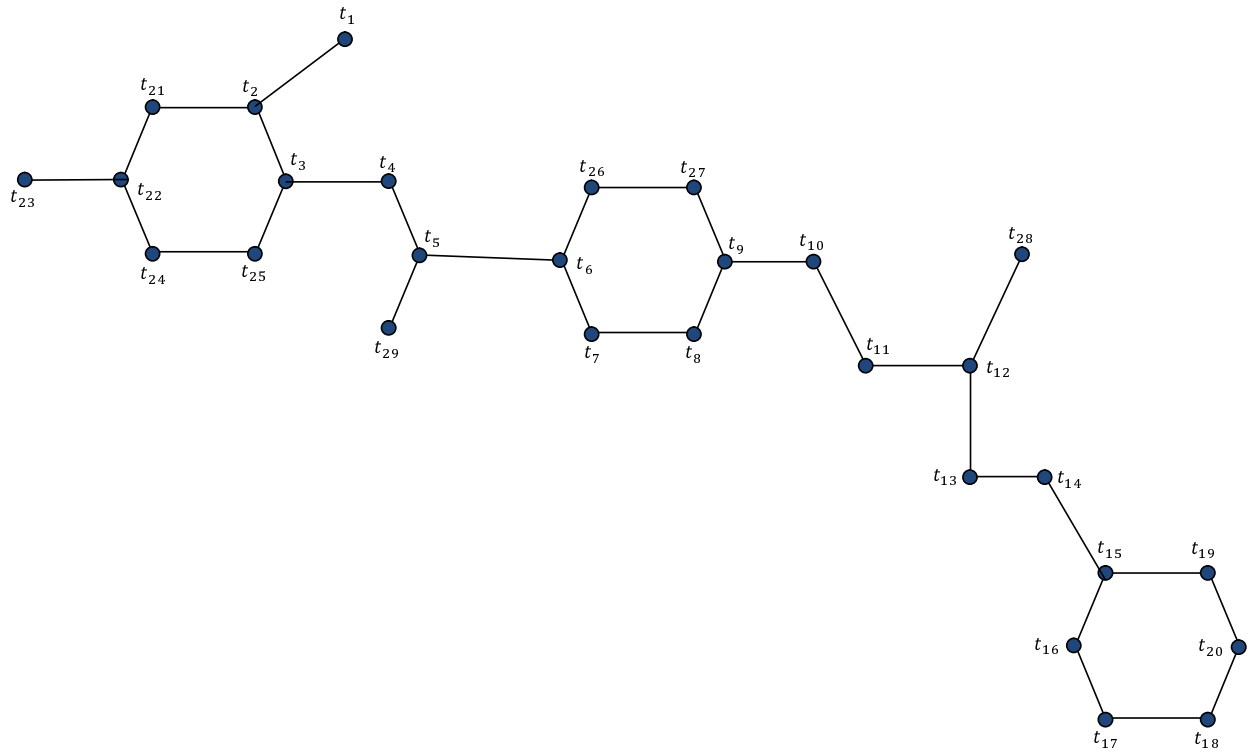

Figure 10. The tucidinostat's chemical graph

$$\delta_r = \begin{cases} 1, & r \in \{1, 19, 27\}, \\ 0, & r \notin \{1, 19, 27\}. \end{cases}$$

In identification $r(t_r \mid \pi)$, each vertex of the tucidinostat drug structure is uniquely determined and thus satisfies the conditions of a partition resolving set. Consequently, the partition resolving number of the graph corresponding to the tucidinostat drug structure is $pd(G_{Tucidinostat}) \leq 3$. By Theorem 2.6, we have $pd(G_{Tucidinostat}) \geq 3$. Combining this result with the previously established upper bound, we conclude that $pd(G_{Tucidinostat}) = 3$.

Theorem 3.5. *Let $G_{Triciferol}$ be a novel drug structure then, $pd(G_{Triciferol}) \leq 4$.*

Proof. The molecular graph of Triciferol consists of 31 vertices (its order) and 33 edges (its size). The set of vertices and edges in the drug structure of triciferol is specified by $V(G_{Triciferol}) = \{f_r : 1 \leq r \leq 31\}$, $E(G_{Triciferol}) = \{f_r f_{r+1} : 1 \leq r \leq 17\} \cup \{f_r f_{r+1} : 19 \leq r \leq 20\} \cup \{f_r f_{r+1} : 22 \leq r \leq 23\} \cup \{f_7 f_{19}\} \cup \{f_9 f_{21}\} \cup \{f_9 f_{28}\} \cup \{f_{11} f_{29}\} \cup \{f_{13} f_{30}\} \cup \{f_{16} f_{31}\} \cup \{f_8 f_{26}\} \cup \{f_{10} f_{27}\} \cup \{f_{26} f_{27}\} \cup \{f_2 f_{22}\} \cup \{f_4 f_{24}\} \cup$

Table 6. Representation of each node of Tudidinostat with respect π

$r(t_r\|\pi)$	π_1	π_2	π_3	Range
t_r	0	7	δ_r	$r=1$
t_r	$r-1$	$n-21-r$	0	$2\leq r\leq 6$
t_r	$r-1$	$n-19-r$	0	$7\leq r\leq 8$
t_r	$r-1$	$n+r-37$	0	$9\leq r\leq 12$
t_r	$r-1$	$n-13-r$	0	$13\leq r\leq 14$
t_r	$r-1$	$n+r-43$	0	$15\leq r\leq 17$
t_r	$r-1$	2	0	$r=18$
t_r	$r-4$	0	δ_r	$r=19$
t_r	$r-4$	1	0	$r=20$
t_r	$n+r-48$	$n+r-43$	0	$21\leq r\leq 23$
t_r	$n-r-1$	$n+2-r$	0	$24\leq r\leq 25$
t_r	$r-20$	1	0	$r=26$
t_r	$r-20$	0	δ_r	$r=27$
t_r	12	5	0	$r=28$
t_r	5	4	0	$r=29$

$\{f_{23}f_{25}\}$.

Table 7. Representation of each node of Triciferol with respect π

$r(f_r\|\pi)$	π_1	π_2	π_3	π_4	Range
f_r	0	17	9	δ_r	$r=1$
f_r	$r-1$	$n-13-r$	$n-21-r$	0	$2\leq r\leq 9$
f_r	$r-1$	$n-13-r$	$n-39+r$	0	$10\leq r\leq 17$
f_r	17	0	10	δ_r	$r=18$
f_r	$n+r-43$	$n-r$	$n-r-8$	0	$19\leq r\leq 21$
f_r	$n+r-51$	$n+8-r$	$n-r$	0	$22\leq r\leq 24$
f_r	4	17	9	0	$r=25$
f_r	$n+r-49$	$n+5-r$	3	0	$26\leq r\leq 27$
f_r	9	10	0	δ_r	$r=28$
f_r	11	8	4	0	$r=29$
f_r	13	6	6	0	$r=30$
f_r	16	3	9	0	$r=31$

Further, the chemical graph of Triciferol and the vertex labeling used to demonstrate our main findings are shown in Figure 11. As a result, $G_{\text{Triciferol}}$'s partition resolving number is equal to or less than 4.

Let $\pi=\{\pi_1,\pi_2,\pi_3,\pi_4\}$, where $\pi_1=\{f_1\}$, $\pi_2=\{f_{18}\}$, $\pi_3=\{f_{28}\}$, and $\pi_4=V(G_{\text{Triciferol}})\setminus(\pi_1\cup\pi_2\cup\pi_3)$. We claim that π forms a partition resolving set for the graph $G_{\text{Triciferol}}$. To justify this, it is sufficient to show that every vertex f_r, for $1\leq r\leq 31$, admits a unique representation with respect to π. The corresponding representations f_r of the vertices of $G_{\text{Triciferol}}$, for $1\leq r\leq 31$, are listed in Table 7.

$$\delta_r=\begin{cases}1, & r\in\{1,18,28\},\\ 0, & r\notin\{1,18,28\}.\end{cases}$$

In identification $r(f_r\mid\pi)$, each vertex of the triciferol drug structure is uniquely determined and thus satisfies the conditions of a partition resolving set. Consequently, the partition resolving number of the graph corresponding to the triciferol drug structure is $pd(G_{Tricifierol})\leq 4$.

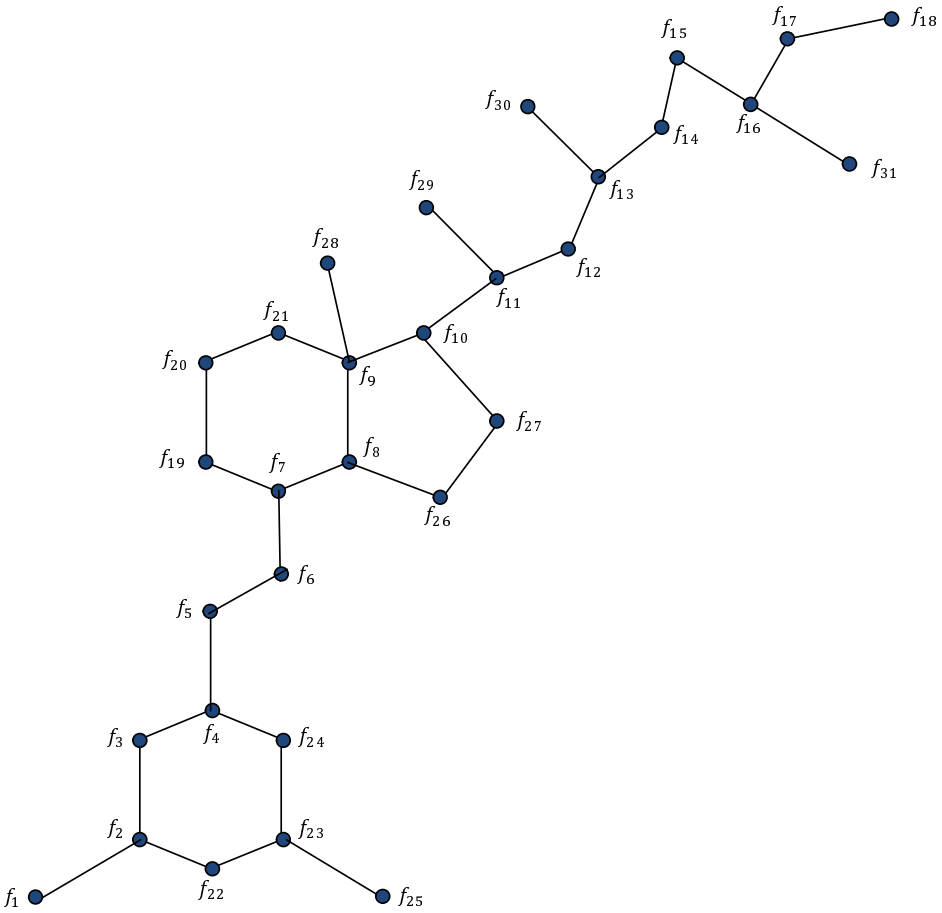

Figure 11. The Triciferol's chemical graph

4. Final observation

The analysis reveals that the partition dimension of the molecular graphs corresponding to CUDC-101, Vorinostat and Tucidinostat is equal to 3, indicating that a minimal set of three resolving partitions is sufficient to uniquely distinguish all vertices in these structures. This reflects a comparatively balanced molecular architecture with moderate symmetry and well-distributed functional groups. On the other hand, the partition dimension of CUDC-907 and Triciferol has been noted to reach at least value smaller than or equal to four which indicates an even higher level of structural complexity, and an even higher level of entailing a vertex indistinguishability due to further researched branching or asymmetry. The obtained results demonstrate that partition resolving sets can serve as an efficient mathematical tool for structural identification in chemical networks. Such representations may contribute to applications in computational chemistry, molecular structure comparison, drug database indexing, and navigation in molecular networks used in drug discovery and design. The consequences of these findings highlight the sensitivity of the partition dimension to the minute differences in molecular topology, which supports the use of the partition dimension as a distance-based measure used to discriminate between anticancer drug structures common therapeutic attributes but with divergent chemical structure. These findings have been briefly summarized in Table 8.

Table 8. Overview of the results

Graphs	Partition Resolving Number $[pd(G)]$
$G_{CUDC-101}$	3
$G_{CUDC907}$	≤ 4
$G_{Vorinostat}$	3
$G_{Tucidinostat}$	3
$G_{Triciferol}$	≤ 4

5. Concluding Remarks and Future Research

The obtained partition dimension values provide insight into the structural organization of the considered drug molecular graphs from a graph-theoretical perspective. A larger partition dimension indicates that a more refined resolving partition is required to uniquely distinguish all vertices, reflecting a comparatively more intricate structural arrangement of the molecular graph. Conversely, a smaller partition dimension suggests that fewer partition classes are sufficient to uniquely identify the vertices through their distance representations. Thus, the partition dimension serves as an effective distance-based graph invariant for characterizing the structural complexity of molecular graphs. The results presented in this work extend the study of partition dimension to anticancer drug molecular graphs and provide a mathematical foundation for future investigations involving other classes of drug molecules and their graph-theoretical properties. The partition dimension of several anticancer medication compounds that have previously been described, namely CUDC101, CUDC 907, Triciferol, Vorinostat and Tucidinostat were studied using a strict graph-theoretic model. The drug molecules were represented as a molecular graph wherein atoms were represented as a vertex and chemical bond as edges which gave a sound platform on which their intrinsic structural properties could be analyzed. By working up the properly adjusted resolving partitions we could find out the precise values of the dimensions of partitions or, in cases where precise values were not available, could provide close bounds. The results of this analysis reveal that the dimension of partition is strongly affected by the molecular architecture underlining it including its symmetries, patterns of branching, and the presence of functional groups. These structural characteristics are determinative towards distinguishing between the vertices and make significant contributions to the topological complexity that is apparent in the drugs molecules at large.

6. Limitations.

The present study is limited to the graph-theoretical analysis of hydrogen-suppressed molecular graphs and does not investigate correlations between the partition dimension and the biological activity or physicochemical properties of the considered anticancer drugs. Consequently, the results provide mathematical characterization of the molecular structures rather than direct chemical or pharmacological interpretations.

7. Discussion

The obtained resolving partition dimensions reflect the structural characteristics of the corresponding molecular graphs. In these graphs, atoms are represented as vertices and chemical bonds as edges. The presence of fused rings creates highly symmetric regions, where several vertices have similar distance relationships. Consequently, additional partition classes are required to distinguish these vertices uniquely, resulting in the computed resolving partition dimension. On the other hand, branching and terminal atoms introduce asymmetry into the molecular graph, producing distinct distance representations that facilitate vertex identification with fewer partition classes.

Therefore, the resolving partition dimension depends not only on the number of vertices but also on the arrangement of rings, branches, and the overall connectivity of the molecular graph. The computed partition dimensions demonstrate that the selected partition sets are sufficient to uniquely identify every atom in the molecular structure. These findings establish a meaningful connection between graph-theoretical resolving partitions and the underlying chemical topology, indicating that resolving partition dimension can serve as a useful descriptor for analyzing the structural complexity of molecular graphs.

The metric dimension and edge metric dimension of CUDC-101 and Vorinostat are 2, whereas the partition dimension is 3. Similarly, Triciferol and CUDC-907 require a larger partition dimension than their metric dimensions, indicating that resolving partitions generally require more structural information than resolving sets. These observations demonstrate that the partition dimension is a distinct graph invariant that complements other distance-based invariants while preserving the objective of uniquely distinguishing the vertices of molecular graphs.

Graph-theoretic resolvability parameters, including the partition dimension, provide mathematical descriptors that uniquely distinguish the vertices of molecular graphs through distance representations. Such descriptors have potential applications in cheminformatics, including molecular graph indexing, structural identification, similarity analysis, and the organization of chemical databases. Since each vertex is assigned a unique distance representation with respect to a resolving partition, partition dimension can support efficient identification and characterization of molecular structures. Although the present work focuses on establishing the partition dimensions of anticancer drug molecular graphs, the computed results may serve as a theoretical foundation for future studies exploring practical cheminformatics applications and the integration of graph invariants into molecular analysis methods.

Open Problem. Determine whether the partition dimensions of the molecular graphs corresponding to CUDC-907 and Triciferol are equal to 3 or 4.

Acknowledgment

This research was supported by the University of Phayao and the Thailand Science Research and Innovation Fund (Fundamental Fund 2027)

REFERENCES

1. PubChem, an open chemistry database at the National Institutes of Health (NIH), https://pubchem.ncbi.nlm.nih.gov/. (2021).
2. R. Jenke, N. Rebing, F. K. Hansen, A. Aigner, and T. Buch, Anticancer Therapy with HDAC Inhibitors: Mechanism-Based Combination Strategies and Future Perspectives, $Cancers(Basel)$. 2021, 13(4), 634.
3. K. W. Kennath, and L.W. Fu, CUDC-907, a dual HDAC and PI3K inhibitor, reverses platinum drug resistance, $Investigational\ new\ drugs$, 2018, 36(1), 10–19.
4. L. E. Tavera , Mendoza, T. D. Quach, B. Dabbas, J. Hudon, X. Liao, A. Palijan, J. L. Gleason, and J. H. White, Function Histone Deacetylase 6 as a cofactor of nuclear, $Journal\ of\ Biological\ Chemistry$, Proc. Natl. Acad. Sci. 2008, 105, 8250.
5. Chemspider, Search and share chemistry, http://www.chemspider.com/AboutUs.aspx. (2021).
6. A. Ali, W. Nazeer, M. Munir, and S. M. Kang, M-polynomials and topological indices of zigzagand rhombic benzenoid systems, $Open\ Chemistry$., 16 (2018), 122–135.
7. M. K. Jamil, M. Imran, and K. A. Sattar, Novel face index for benzenoid hydrocarbons, $Mathematics$, 8 (2020), 312.
8. M. K. Siddiqui, M. Naeem, N. A. Rahman, and M. Imran, Computing topological indices of certain networks, $Journal\ of\ Optoelectronics\ and\ Advanced\ Materials$, 18 (2016), 9–10.
9. F. M. Nadeem, M. Azeem, and H. A. Siddiqui, Comparative study of zagreb indices for capped, semi-capped, and uncapped carbon nanotubes, $Polycyclic\ Aromatic\ Compound$, (2020), 1–18.
10. M. F. Nadeem, M. Imran, H. M. A. Siddiqui, M. Azeem, A. Khalil, and Y. Ali, Topological aspects of metal-organic structure with the help of underlying networks, $Arabian\ Journal\ of\ Chemistry$, 14 (2021), 103157.
11. D. H. Trong, V. K. H. Le, and T. P. D. Pham, Delivery systems for vorinostat in cancer treatment: An updated review. $Journal\ of\ Drug\ Delivery\ Science\ and\ Technology$, 61 (2021), 102334.
12. Y. Sun, J. H. Hong, Z. Ning, D. Pan, X. Fu, X. Lu and J. Tan, Therapeutic potential of tucidinostat, a subtype-selective histone deacetylase inhibitor, in hematological malignancies and solid tumors. $Frontiers\ in\ Pharmacology$, 13, (2022) 932914.
13. S. Fortin, and G. Berube, Advances in the development of hybrid anticancer drugs. $Expert\ Opinion\ on\ Drug\ Discovery$, 8(9) (2013) , 1029–1047.
14. C. J. Lai, R. Bao, X. Tao, J. Wang, R. Atoyan, H. Qu, G. G. Wang, L. Yin, M. Samson, J. Forrester, B. Zifcak, G. X. Xu, D. DellaRocca, H. X. Zhai, X. Cai, W. E. Munger, M. Keegan, C. V. Pepicelli, and C. Qian, CUDC-101, a multitargeted inhibitor of

histone deacetylase, epidermal growth factor receptor, and human epidermal growth factor receptor 2, exerts potent anticancer activity. $CancerRes$, 70(9), (2010), 3647-56.
15. L. Hegedus, S. Qaisieh, C. Stulpnagel, Y. G. K. Dezfouli, W. Tambo, F. Doerr, and S. Bolukbas, Dual HDAC and PI3K Inhibitor CUDC-907 Inhibits Growth of Pleural Mesothelioma: The Impact of Cisplatin Sensitivity and Myc Expression. $Cells$, 14(20), (2025), 1599.
16. P.J. Slater, Leaves of trees, Southeastern Conference on Combinatorics, Graph Theory, and Computing, $Congressus\ Numerantium$, 14 (1975), 549–559.
17. F. Harary, and R.A. Melter, On the metric dimension of a graph, $Ars\ Combinatoria$. 2 (1976), 191–195.
18. G. Chartrand, E. Salehi, and P. Zhang, The partition dimension of graph, $Aequationes\ mathematicae$, 59, (2000), 45–54.
19. G. Chartrand, L. Eroh, M. A. O. Johnson, and R. Ortrud, Resolvability in graphs and the metric dimension of a graph, $Discrete\ Applied\ Mathematics$, 105 (2000), 99–113.
20. S. Khuller, B. Raghavachari, and A. Rosenfeld, Landmarks in graphs, $DiscreteApplied.Mathematics$, 70 (1996), 217–229.
21. M. F. Nadeem, M. Hassan, M. Azeem, S. U. Khan, M. R. Shaik, and M. A. F. Sharaf, Application of resolvability technique to investigate the different polyphenyl structures for polymer industry, $Journal\ of\ Chemistry$, (2021).
22. A. Ahmad, A. N. A. Koam, M. H. F. Siddiqui, and M. Azeem, Resolvability of the starphene structure and applications in electronics, $Ain\ Shams\ Engineering\ Journal$, 13 (2022), 101587.
23. A. Sebo, E. Tannier, On metric generators of graphs, $Mathmatics\ of\ Operation\ Research$, 29 (2004), 191–406.
24. J. B. Liu, M. F. Nadeem, and M. Azeem, Bounds on the partition dimension of convex polytopes, $Combinatorial\ Chemistry\ \&\ High\ Throughput\ Screening$, 25, (2020), 547–553.
25. M. Azeem, M. Imran, and M. F. Nadeem, Sharp bounds on partition dimension of hexagonal mobius ladder, $Journal\ of\ King\ Saud\ University$, 34 (2022), 101779.
26. N. Mehreen, R. Farooq, and S. Akhter, On partition dimension of fullerene graphs, $AIMS\ Mathematics$, 3, (2018), 343–352.
27. A. Shabbir,and M. Azeem, On the partition dimension of tri-hexagonal alpha-boron nanotube, $IEEE Access$, 9 (2021), 55644–55653.
28. M. K. Siddiqui, and M. Imran, Computing the metric and partition dimension of h-naphtalenic and $vc5c_7$ nanotubes, $Journal\ of\ Optoelectronics\ and\ Advanced\ Materials$, 17 (2015), 790–794.
29. H. M. A. Siddiqui, and M. Imran, Computing metric and partition dimension of 2-dimensional lattices of certain nanotubes, $Journal\ of\ Computational\ and\ Theoretical\ Nanoscience$, 11 (2014), 2419–2423.
30. Y. Listiana, L. Susilowati, S. Slamin, and K. Dliou, Some Properties of the Central Local Metric Dimension on Corona Product Graphs, $Statistics\ Optimization\ and\ Informization\ Computing$, 15, (2026), 3668-3677.
31. R. Umilasari, L. Susilowati, S. Afadekemi, J. Osaye, and I. Saifudin, Some Properties of Dominant Local Metric Dimension, $Statistics\ Optimization\ and\ Informization\ Computing$, 12, 2024, 1912–1920.
32. A. A. Khabyah, M. K. Jami, A. N. A. Koam, A. Javed and M. Azeem, Partition dimension of COVID antiviral drug structures, $Mathematical\ Bioscience\ and\ Engineering$, 2022, 10078–10095.
33. Q. Huang, A. Khalil, D. A. Ali, A. Ahmad, R. Luo and M. Azeem, Breast cancer chemical structures and their partition resolvability, $Mathematical\ Bioscience\ and\ Engineering$, 2022, 3838–3853.
34. E. C. M. Maritz, and T. Vetrik, The partition dimension of circulant graphs, $Quaestiones\ Mathematicae$, 41 (2018), 49–63.
35. Z. Hussain, S. Kang, M. Rafique, M. Munir, U. Ali, and A. Zahid, Bounds for partition dimension of m-wheels, $Open\ Physics$, 17 (2019), 340–344.
36. Amrullah, E. T. Baskoro, R. Simanjuntak, and S. Uttunggadewa, The partition dimension of a subdivision of a complete graph, $Procedia\ Computer\ Science$, 74 (2015), 53–59.
37. C. Wei, M. F. Nadeem, H. M. A. Siddiqui, M. Azeem, J. B. Liu, and A. Khalil, On partition dimension of some cycle-related graphs, $Mathematical\ Problems\ in\ Engineering$, 2021 (2021), 4046909.
38. J. Santoso and Darmaji, The partition dimension of cycle books graph , $Journal\ of\ Physics\ Conference\ Series$, 974, (2018), 012070.
39. Darmaji, and R. Alfarisi, On the partition dimension of comb product of path and complete graph, $AIP\ Conference\ Proceedings$, (2017), 020038.
40. A. Nadeem, A. Kashif, S. Zafar, and Z. Zahid, On 2-partition dimension of the circulant graphs, $Journal\ of\ Intelligentand\ Fuzzy\ Systems$, 40 (2021), 9493–9503.